An analytic approach to the hydrogen Stark effect in weak, strong, and ultrastrong fields*

Jess Fauchier† and John D. Dow
Department of Physics and Materials Research Laboratory, University of Illinois at Urbana-Champaign, Urbana, Illinois 61801
(Received 18 May 1973)

An accurate analytic approximate solution of the hydrogen-Stark-effect Schrödinger equation is obtained. In contrast to previous non-numerical solutions, this solution (which is piecewise continuous, and easily calculable) is accurate for applied electric fields of arbitrary strength—including weak fields ($F \lesssim 0.1F_{\text{ion}}$; the Stark-shift regime), strong fields ($F \lesssim F_{\text{ion}}$), and ultrastrong fields ($F \gtrsim 10^2 F_{\text{ion}}$), where $F_{\text{ion}} = 3 \times 10^8$ V/cm is the classical ionization field of hydrogen. The ultrastrong-field regime is experimentally accessible in solid-state physics where, for hydrogenic excitons, F_{ion} may be as small as 10^2 V/cm.

I. INTRODUCTION

The application of quantum-mechanical perturbation theory to Schrödinger's equation occupies a central role in modern theoretical physics. Of particular interest are unbounded perturbations, which qualitatively modify the unperturbed wave functions and often qualitatively alter the spectrum of the Hamiltonian.[1] A classic prototype of a single-particle Schrödinger equation with an unbounded perturbation is the Stark effect in hydrogen, which is described by the unperturbed Hamiltonian

$$\mathcal{H}_0 = (-\hbar^2/2m)\nabla^2 - Ze^2/(\epsilon_0 r), \tag{1.1}$$

the perturbation

$$V(\vec{\mathbf{r}}) = -eFz, \tag{1.2}$$

and the Schrödinger equation

$$\mathcal{H}\psi(\vec{\mathbf{r}}) = (\mathcal{H}_0 + V)\psi(\vec{\mathbf{r}}) = E\psi(\vec{\mathbf{r}}). \tag{1.3}$$

Here e and m are the electron's charge and reduced mass, F is the magnitude of the constant applied electric field, and the Cartesian coordinate system has been chosen such that $\vec{\mathbf{F}}$ is directed along the z axis. For hydrogen, Z and ϵ_0 are unity, and we use Gaussian cgs units.

The spectrum of the unperturbed hydrogenic Hamiltonian contains the usual continuum of unbound positive energy states together with the n^2-fold-degenerate bound Rydberg states of energy

$$E_n = -R/n^2 \quad (n = 1, 2, 3, \ldots),$$

where $2\pi\hbar$ is Planck's constant and R is the Rydberg

$$R = me^4/(2\epsilon_0^2\hbar^2). \tag{1.4}$$

The application of a small but finite field $\vec{\mathbf{F}}$ shifts and splits the bound-state levels, as discussed in elementary quantum-mechanics textbooks. However, in addition to shifting and splitting levels, the field also broadens them, introducing a continuous density of negative-energy perturbed states in place of the countable infinity of discrete bound unperturbed states. Physically, the broadening is a consequence of field ionization of the hydrogen atom: since an electron wavepacket, with energy E and initially localized near the proton, can tunnel into a distant classically allowed region where r and z are such that $-eFz - e^2/\epsilon_0 r < E$. Thus in a uniform electric field the hydrogen atom has no bound states, the formerly bound zero-field levels being reduced to quasibound resonance states as the field introduces a continuum of negative-energy states. (For weak fields, the probability of finding an electron near the proton in one of these formerly forbidden negative-energy levels is tiny.)

Of course, electric fields found in nature are neither arbitrarily uniform nor arbitrarily large; still Rausch von Traubenberg was able to demonstrate the importance of field broadening in the spectrum of hydrogen as early as 1929.[2]

A theory of the field ionization was first proposed by Oppenheimer in 1928,[3] using what has come to be known as the tunneling Hamiltonian approach.[4] Subsequently, Lanczos and others developed semiclassical WKB approximations to the Stark-effect solutions[5-7]; more recent theoretical developments have dealt with the field dependences of the energies, the widths, and the strengths of the perturbed spectral lines.[8-12]

Virtually all these theories of the hydrogen Stark effect are meant to be applied to the weak-field regime $f \lesssim 0.1$, where we have

$$f = |e|Fa/R, \tag{1.5}$$

and a is the Bohr radius

$$a=\hbar^2\epsilon_0/me^2. \tag{1.6}$$

For hydrogen in a vacuum, $f=1$ corresponds to a field of 2.57×10^9 V/cm and to a field of $\frac{1}{2}$ a.u., with $a=1$, $R=\frac{1}{2}$. Note that f is the ratio of the applied-field potential energy drop across the $1s$ radius to the $1s$ binding energy. The nth bound state is fully ionized whenever $fn^4\gtrsim 1$. For hydrogen, $f=0.125$ is the classical ionization field of the $1s$ level, whereas uniform static fields such that $f\gtrsim 1$ are generally inaccessible in the laboratory. However, nonuniform time-varying fields larger than $f=1$ are produced by highly ionized plasmas and by high-powered lasers; thus a study of the ultrastrong constant-field Stark effect may be regarded as a first step toward understanding the physics of atoms in intense plasma and laser fields.

Recently, an experimental situation has arisen in which the ultrastrong-field hydrogenic Stark effect ($f\gg 0.1$) is accessible; this is the optical absorption by weak-binding excitons in an electric field.[13,14] An exciton in a high-resistivity covalent semiconductor consists of an extra electron in the empty conduction band interacting with a hole in the filled valence band. Both electron and hole interact with an external electric field and with each other. In the effective-mass approximation,[15] the internal motion of the exciton is governed by the same Schrödinger equation as the hydrogen atom—except the effective mass m may be as small as $0.01m_0$ (where m_0 is the free-electron mass) and the static dielectric constant is typically $\epsilon_0\approx 15$. Thus, in contrast to the hydrogen atom, the exciton is extremely polarizable and can be easily and completely ionized by applied fields as small as 10^3 V/cm.

For the most part, theoretical treatments of the strong-field electroabsorption by excitons[14,16-18] have ignored perturbative and semiclassical approximations, and have solved the perturbed Schrödinger equation [Eq. (1.3)] numerically. The present work attempts to bridge the gap between the existing (but cumbersome) strong-field numerical work and the simpler moderate-field analytical treatments of the hydrogen Stark effect. The primary new result of this paper is the construction of *quantitatively accurate and analytically simple* wave functions for a hydrogen atom subjected to a uniform electric field of arbitrary strength. The methods used in achieving such wave functions are not new, and are related to semiclassical WKB approximations used by other authors.[3,5-10,12]

Accurate strong-field expressions for the hydrogenic wave functions greatly simplify the (numerically difficult) evaluation of indirect electroabsorption spectra[19]; calculations of cross sections for all processes involving the scattering of field-perturbed excitons are facilitated by the existence of accurate approximate wave functions. Furthermore, a better understanding of the strong-field limit is essential to a complete understanding of the Stark perturbation series.

In Sec. II, a general discussion of the hydrogen Stark-effect problem and its solution is given. Sections III and IV contain the details of the Stark-effect wave functions. The results of the theory are discussed in Sec. V, while Sec. VI contains the conclusions.

II. GENERAL

Taking units of energy and length to be the Rydberg and Bohr radius and writing

$$\Psi^{\mathrm{UN}}(\mathbf{r})=(\xi\eta)^{-1/2}\chi_1(\xi)\chi_2(\eta)e^{im\varphi}\quad(m=0,\pm1,\pm2,\ldots), \tag{2.1}$$

where (ξ,η,φ) are parabolic coordinates

$$\xi=r+z, \tag{2.2}$$

$$\eta=r-z, \tag{2.3}$$

$$\varphi=\varphi, \tag{2.4}$$

we find the separated equations of motion for an electron orbiting a fixed nucleus of charge $-Ze$ in a field F:

$$\left[\frac{-d^2}{d\xi^2}+\left(\frac{m^2-1}{4\xi^2}-\frac{t}{\xi}-\frac{E}{4}+\frac{f\xi}{8}\right)\right]\chi_1(\xi)=0, \tag{2.5}$$

$$\left[\frac{-d^2}{d\eta^2}+\left(\frac{m^2-1}{4\eta^2}-\frac{(Z-t)}{\eta}-\frac{E}{4}-\frac{f\eta}{8}\right)\right]\chi_2(\eta)=0. \tag{2.6}$$

In Eq. (2.1), we have used the superscript UN to emphasize that the wave function Ψ^{UN} is unnormalized and subject to the boundary conditions

$$\chi_1(\xi)=\xi^{(1+|m|)/2}[1-\xi t/(1+|m|)+O(\xi^2)], \tag{2.7}$$

$$\chi_1(\xi)=[-E/f+\xi/2]^{-1/4}\times\exp[-\tfrac{2}{3}f^{1/2}(-E/f+\xi/2)^{3/2}]\quad\text{for }\xi\to\infty, \tag{2.8}$$

$$\chi_2(\eta)=\eta^{(1+|m|)/2}\times[(1-\eta(Z-t)/(1+|m|)+O(\eta^2)], \tag{2.9}$$

and

$$\chi_2(\eta)=\frac{\mathfrak{C}(E,Z,f)}{[E/f+\eta/2]^{1/4}}\times\sin\left[\tfrac{2}{3}f^{1/2}\left(\frac{E}{f}+\frac{\eta}{2}\right)^{3/2}+\gamma\right]\quad\text{for }\eta\to\infty. \tag{2.10}$$

Here $O(x^2)$ means terms of order x^2 or higher. Of course, the normalized wave function is simply

$$\Psi(\vec{r}) = \frac{\Psi^{UN}(\vec{r})}{\left[\int |\Psi^{UN}(\vec{r})|^2 d^3r\right]^{1/2}} = \frac{(\xi\eta)^{-1/2}\chi_1(\xi)\chi_2(\eta)e^{im\varphi}}{\pi^{1/2}(\frac{1}{2}f)^{1/4}\mathfrak{N}^{1/2}(E,f)\mathfrak{G}(E,Z,f)} \tag{2.11}$$

where we have

$$\mathfrak{N}(E,f) = \int_0^\infty [\chi_1^2(\xi)/\xi]\, d\xi\,. \tag{2.12}$$

The above separation of the Stark-effect problem in parabolic coordinates was studied in the early days of quantum mechanics by Schrödinger, Epstein, Fock, and Bargmann.[20] The eigenvalue of the equation (2.6) for χ_2 is the energy E, which has a continuous spectrum of positive and negative energies; t is the eigenvalue of the equation (2.5) for χ_1, and has a discrete set of values $t_N(E)$, where N $(=0, 1, 2, \ldots)$ is the number of nodes of $\chi_1(\xi; t_N)$.

It is desirable to have a single function to characterize the quality of an approximate solution of the equations of motion; this function should be sensitive to the behavior of the electron's wave function both near the hydrogen nucleus and far from it. We choose the "absorption function" $\epsilon_2(E)$,

$$\epsilon_2(E;f) \equiv \lim_{\vec{r}\to 0} \sum_\nu |\Psi_\nu(\vec{r};f)|^2 \delta(E-E_\nu) = -\pi^{-1}\mathrm{Im}\lim_{\vec{r},\vec{r}'\to 0} G(\vec{r},\vec{r}',E), \tag{2.13}$$

because it is such a function, and because it is essentially the optical-absorption spectrum for excitons in an electric field $\vec{F}$. Here the quantum numbers of the stationary states of Eq. (2.5) are labeled by ν, and $\delta(x)$ is the Dirac δ function.

It follows that $\epsilon_2(E)$ is

$$\epsilon_2(E;f) = \sum_\nu |\Psi_\nu(0)|^2 \delta(E-E_\nu)\,, \tag{2.14}$$

$$= \left(\frac{2}{\pi^2 f}\right)^{1/2} \sum_{N=0}^{\infty} \mathfrak{N}_N^{-1}(E,f)\mathfrak{G}_N^{-2}(E,Z,f) \tag{2.15}$$

and depends on three factors:
(1) $\mathfrak{N}(E,f)$, the bound-state normalization factor for χ_1;
(2) $\mathfrak{G}(E,Z,f)$, the continuum "normalization" factor for χ_2; and
(3) $t_N(E,f)$, the eigenvalue which implicitly determines the values of $\mathfrak{N}$ and $\mathfrak{G}$ above.

It is noteworthy that all of the dynamical information of the Stark-effect problem is contained in the Green's function $G(\vec{r},\vec{r}',E)$ of Eq. (2.13); any observable property of a (spinless) hydrogen atom in an electric field can be evaluated once the Green's function has been determined. Furthermore existing non-numerical Stark-effect solutions are incapable of reproducing the qualitative features of either $G(\vec{r},\vec{r}',E)$ or $\epsilon_2(E;f)$ except in the small-field perturbation limit $f \to 0$.

The evaluation of the factors $\mathfrak{N}$ and $\mathfrak{G}$ in the function $\epsilon_2(E;f)$ is greatly simplified by a change of scale

$$u = f^{1/3}\xi\,, \tag{2.16}$$

$$v = f^{1/3}\eta\,. \tag{2.17}$$

The resulting equations of motion are

$$\left(-\frac{d^2}{du^2} + \frac{m^2-1}{4u^2} - \frac{\tau}{u} - \frac{E'}{4} + \frac{u}{8}\right)\chi_1(u) = 0 \tag{2.18}$$

and

$$\left(-\frac{d^2}{dv^2} + \frac{m^2-1}{4v^2} - \frac{T}{v} - \frac{E'}{4} - \frac{v}{8}\right)\chi_2(v) = 0\,. \tag{2.19}$$

Here we have

$$E' \equiv E/f^{2/3}\,, \tag{2.20}$$

$$\tau_N(E') \equiv f^{-1/3}t_N(E,f)\,, \tag{2.21}$$

and

$$T_N(E',Z') = f^{-1/3}Z - \tau_N(E') \tag{2.22}$$

$$\equiv Z' - \tau_N(E')\,. \tag{2.23}$$

In solving Eqs. (2.18) and (2.19), we fix the energy E' and the number of nodes N and note that only solutions with $m=0$ contribute to $\epsilon_2(E)$. First, the eigenvalue $\tau_N(E')$ is determined, and used to compute $\mathfrak{N}_N(E')$. Given τ_N and a particular value of $Z' = Z/f^{2/3}$, T_N is determined by Eq. (2.22), permitting solution of Eq. (2.19) for χ_2 and $\mathfrak{G}_N(E', Z')$. The scaling relations

$$\mathfrak{N}(E,f) = \mathfrak{N}(E/f^{2/3}, 1) \tag{2.24}$$

and

$$\mathfrak{G}_N(E,Z,f) = f^{-1/6}\mathfrak{G}_N(E/f^{2/3}, Z/f^{1/3}, 1) \tag{2.25}$$

allow computation of $\epsilon_2(E)$ [via Eq. (2.15)] for all values of dimensionless applied strength f in terms of the solutions of Eqs. (2.18) and (2.19).

III. BOUND-STATE EQUATION FOR $\chi_1(u)$

A. General

The bound-state equation

$$\frac{-d^2}{du^2}\chi_1 + U_1(u)\chi_1 = u^{-1}t_N\chi_1 \tag{3.1}$$

is to be solved for the wave function $\chi_1(u; E/f^{2/3}, m, \tau_N)$ and the eigenvalues τ_N. The "partial potential" $U_1(u)$ is

$$U_1(u)=\frac{m^2-1}{4u^2}-\frac{E/f^{2/3}}{4}+\frac{u}{8}, \tag{3.2}$$

and the "classical kinetic energy" $E_{k1}(u)$ is

$$E_{k1}(u)\equiv -U_1(u)+tu^{-1}\equiv -W_1(u) \tag{3.3}$$

where $W_1(u)$ is the effective potential energy. The effective potential energy is depicted in Fig. 1 for the cases of interest.

The approximate solutions are taken to have the form

$$\chi_1(u)=\begin{cases} G^{\rm in}(u;E',\tau) & \text{for } u<u_M \\ A^N(E',\tau)G^{\rm out}(u;E',\tau)+B^N(E',\tau)H^{\rm out}(u;E',\tau) & \end{cases} \tag{3.4}$$

for $u\geq u_M$,

where u_M is a matching point between the inside solution $G^{\rm in}$ and the outside solutions $G^{\rm out}$ and $H^{\rm out}$, and is taken to be

$$u_M=\begin{cases} 1, & \tau>3 \\ 3, & \tau\leq 3. \end{cases} \tag{3.5}$$

The functions $G^{\rm in}$, $G^{\rm out}$, and $H^{\rm out}$ are functions that approximate the solutions of differential equation (3.1) and are regular at the origin, regular at infinity, and irregular at infinity, respectively. The coefficients A^N and B^N are chosen such that the wave function χ_1 and its derivative are continuous at the matching point u_M.

The eigenvalue τ_N is determined by the condition that χ_1 be regular at infinity:

$$B^N(E',\tau_N)=0, \tag{3.6}$$

an equation with a denumerable infinity of solutions $\tau_N(E')$, the number of χ_1's nodes being specified by N $(=0,1,2,\ldots)$.

The normalization of χ_1 is specified analytically, using a method dating back to the early days of quantum theory[21]:

$$\mathfrak{N}_N(E')=-\left(\frac{1}{\pi}\right)\left[A(E',\tau)\left(\frac{d}{d\tau}\right)B(E',\tau)\right]\Big|_{\tau=\tau_N}, \tag{3.7}$$

where $A(E',\tau)$ and $B(E',\tau)$ are specified in Eq. (3.4).

B. Inside wave function $G^{\rm in}(u)$

A power series determines $G^{\rm in}$:

$$G^{\rm in}=u^{(1+|m|)/2}\sum_{\nu=0}^{p}a_\nu u^\nu, \tag{3.8}$$

where

$$a_0=1, \tag{3.9}$$

$$a_1=-\tau \tag{3.10}$$

$$a_2=+\tfrac{1}{4}(\tau^2-\tfrac{1}{4}E), \tag{3.11}$$

and

$$a_\nu=-(\tfrac{1}{2}a_{\nu-3}+E'a_{\nu-2}+4\tau a_{\nu-1})/(4\nu^2), \quad \nu\geq 3. \tag{3.12}$$

The power series is terminated for $\nu=p$, where

$$\left|\sum_{\nu=p-2}^{p}a_\nu u^\nu\right|<\epsilon\left|\sum_{\nu=0}^{p}a_\nu u^\nu\right|, \tag{3.13}$$

and $\epsilon=0.001$.

C. Outside solutions $G^{\rm out}(u)$ and $H^{\rm out}(u)$

In treating the outside solution, we distinguish two cases, depending on whether there are one or three "turning points" u_i [i.e., points at which $E_{k1}(u_i)=0$] (see Fig. 1).

For the case of one turning point, we take WKB-like wave functions[22]

$$G^{\rm out}(u)=[S_1(u)/E_{k1}(u)]^{1/4}{\rm Ai}(-V_1(u)) \tag{3.14}$$

$$H^{\rm out}(u)=[S_1(u)/E_{k1}(u)]^{1/4}{\rm Bi}(-V_1(u)) \tag{3.15}$$

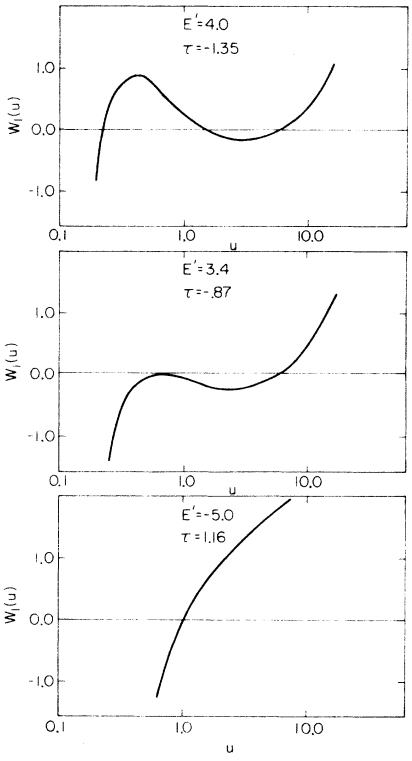

FIG. 1. The effective potential energy $W_1(u)$ (the negative of the classical kinetic energy), defined in Eq. (3.3), for several sets of parameters E' and τ. Case (a) is characteristic of large positive energies, while case (c) corresponds to large negative energies. Case (b) occurs at intermediate energies. Observe that the qualitative features of the kinetic energy, such as the number of classical turning points and the number of maxima and minima, depend upon the energy E'.

where Ai, Bi are Airy functions and $E_{k1}(u)$ is defined in Eq. (3.3). Here we have

$$S_1(u) = \left(\tfrac{3}{2}\int_{u_1}^{u} |E_{k1}(X)|^{1/2} dX\right)^{2/3} \operatorname{sgn}(E_{k1}(u)) \quad (3.16)$$

where sgn is the sign function and u_1 is the turning point. $V_1(u)$ is expressible as

$$V_1(u) = a + bS_1(u), \quad (3.17)$$

with the coefficients a and b given in terms of the derivatives of $E_{k1}(u)$ at the classical turning point u_1 (see Appendix A).

For three turning points, G^{out} and H^{out} are piecewise continuous, having the general WKB form of Eqs. (3.14) and (3.15), but depending in detail on the proximity of u to the various turning points. This case is treated in Appendix A.

IV. CONTINUUM STATE EQUATION FOR $\chi_2(v)$

The continuum state equation

$$\frac{-d^2}{dv^2}\chi_2 + U_2(v)\chi_2 = \tfrac{1}{4}E'\chi_2 \quad (4.1)$$

is to be solved for the wave function $\chi_2(v; E', T_N)$, where T_N, is given in terms of the nuclear charge Z, t_N, and the reduced field f:

$$T_N(E, f, m) = [Z - t_N(E, f, m)]/f^{1/3}. \quad (4.2)$$

The partial potential U_2 is

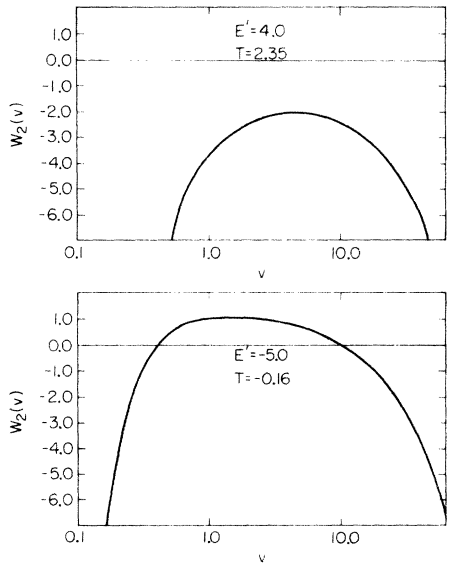

FIG. 2. The effective potential energy $W_2(v)$, (the negative of the classical kinetic energy) defined in Eq. (4.4) plotted for two sets of parameters E' and T. Case (a) is characteristic of large positive E', while case (b) corresponds to large negative E'. Observe that the potential $W_2(v)$ always has one maximum and may have either zero or two zeros [$W_2(v) = 0$] for $m = 0$.

$$U_2(v) = \frac{m^2 - 1}{4v^2} - \frac{T_N}{v} - \frac{v}{8}. \quad (4.3)$$

The effective potential,

$$W_2(v) = -\tfrac{1}{4}E' + U_2(v) \equiv E_{k2}(v), \quad (4.4)$$

is shown in Fig. 2.

Approximate wave functions have the form

$$\chi_2(v) = \begin{cases} K^{\text{in}} & \text{for } v < v_M \\ C^N(E', T_N)K^{\text{out}} + D^N(E', T_N)L^{\text{out}} & \text{for } v > v_M, \end{cases} \quad (4.5)$$

where v_M is a matching point between the inner solution K^{in} and the outer solutions, K^{out} and L^{out}. Note that the matching point v_M must be chosen very carefully to ensure accurate wave functions for all energies. A simple prescription for v_M is

$$v_a = v_0 + \Delta v, \quad (4.6)$$

where v_0 is the (only) extremum of $U_2(v)$,

$$v_M = \begin{cases} 1 & \text{if } t < -5 \\ v_a & \text{if } t > -5 \text{ and } v_a > 1 \\ 1 & \text{if } v_a < 1, \end{cases} \quad (4.7a)$$

where we have

$$v_a = v_0 + \min(\Delta v_1, \Delta v_2), \quad (4.7b)$$

$$\Delta v_1 = |(C_4 - 7C_0C_2/12 + C_0^2/24)/24|^{-0.17}, \quad (4.7c)$$

$$\Delta v_2 = |C_3|^{-0.2}, \quad (4.7d)$$

and

$$c_\nu = \frac{1}{\nu!}\frac{d^\nu}{dv^\nu} E_{k2}(v)\Big|_{v=v_0}. \quad (4.7e)$$

The functions K^{in}, K^{out}, and L^{out} are functions that approximate the solution of the differential Equation (4.1). The inner wave function K^{in} (which is regular at the origin) is determined as the power series (similar to that for G^{in})

$$K^{\text{in}} = v^{(1+m)/2} \sum_{\nu=0}^{p} b_\nu v^\nu, \quad (4.8)$$

where

$$b_0 = 1, \quad (4.9)$$

$$b_1 = -T_N, \quad (4.10)$$

$$b_2 = \tfrac{1}{4}(T_N^2 - \tfrac{1}{4}E'), \quad (4.11)$$

and

$$b_\nu = -[\tfrac{1}{2}b_{\nu-3} + E'b_{\nu-2} + 4T_N b_{\nu-1}]/(4\nu^2). \quad (4.12)$$

The summation is terminated in exactly the same manner as the power-series expression for G^{in} [Eq. (3.13)].

The outer solutions K^{out} and L^{out} are WKB-like, oscillate for large v, and have the asymptotic dependence (with phase shift γ)

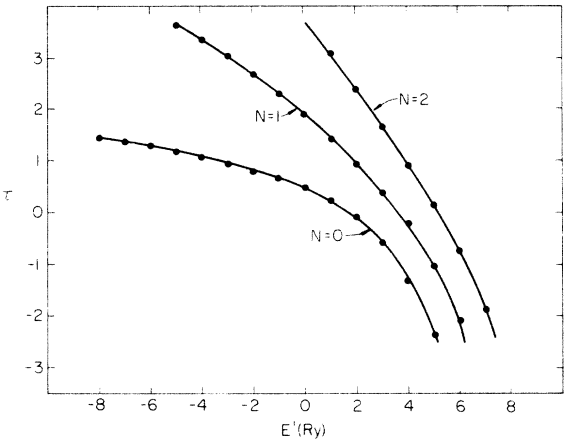

FIG. 3. The eigenvalues τ[Eqs. (2.5) and (2.21)] as functions of the reduced energy $E' = E/f^{2/3}$ for zero, one, and two nodes (N) of the bound-state wave function. Solid line: values obtained by numerical calculation; points: the present theory.

$$K^{\text{out}}(v) = (E' + \tfrac{1}{2}v)^{-1/4} \sin[\tfrac{2}{3}(E' + \tfrac{1}{2}v)^{3/2} + \gamma] , \quad (4.13)$$

$$L^{\text{out}}(v) = (E' + \tfrac{1}{2}v)^{-1/4} \cos[\tfrac{2}{3}(E' + \tfrac{1}{2}v)^{3/2} + \gamma] . \quad (4.14)$$

The exact form of K^{out} and L^{out} depend in detail upon the number of classical turning points and are described in Appendix B.

The coefficients C and D of Eq. (4.5) are chosen to make $\chi_2(v)$ and $(d/dv)\chi_2(v)$ continuous at the matching point v_M. It thus follows from Eqs. (2.10), (4.13), and (4.14) that the amplitude function $\mathfrak{A}$ is given by the expression

$$\mathfrak{A} = \{[C^2(E', T_N) + D^2(E', T_N)]/\pi\}^{1/2} \quad (4.15)$$

which involves only K^{in}, K^{out}, and L^{out} and their derivatives evaluated at v_M.

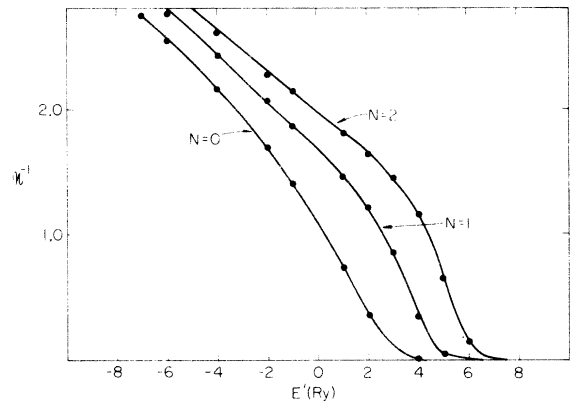

FIG. 4. The reciprocal of the normalization coefficient $\mathfrak{N}$ of the bound-state wave function [Eq. (2.12)], as a function of the reduced energy $E' = E/f^{2/3}$, for values of the node index N of 0, 1, and 2. Points: Present theory; solid lines: numercial results.

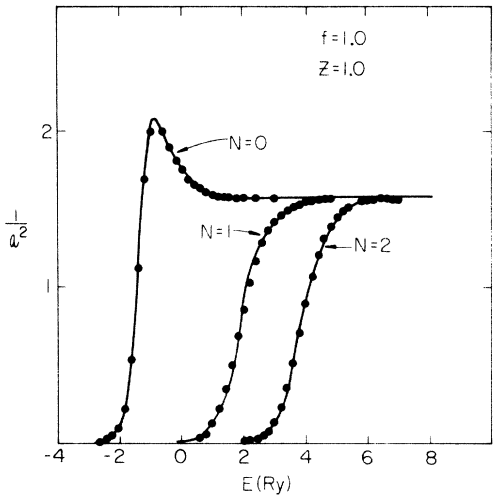

FIG. 5. The square of the reciprocal of $\mathfrak{A}$, the asymptotic amplitude of the continuum wave function [Eq. (2.10)], as a function of the energy, for unit field f and unit charge Z. The number of nodes in the associated bound-state wave function N is 0, 1, or 2. Points: present theory; solid lines: numerical results.

V. RESULTS

The eigenvalues $\tau_N(E')$ and the normalization factors $\mathfrak{N}_N(E')$ computed from the bound-state equation (2.18) are depicted in Figs. 3 and 4 for $N = 0$, 1, and 2 nodes. The agreement with direct numerical computations[23] is excellent.[24]

The amplitude factor $\mathfrak{A}_N(E', Z')$ is plotted in Figs. 5 and 6 for $Z' \equiv Z/f^{2/3} = 1$ and 0 [e.g., hydrogen in unit field and the Franz-Keldysh-effect[13,14]

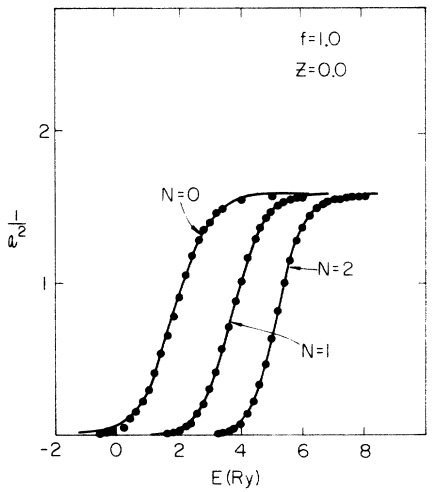

FIG. 6. The reciprocal of the square of the asymptotic amplitude of the continuum wave function in the Franz-Keldysh limit ($Z = 0$), shown as a function of energy, node. The field is taken to be unity, and the node index N takes the values 0, 1, and 2. Points: current theory; solid lines: numerical results.

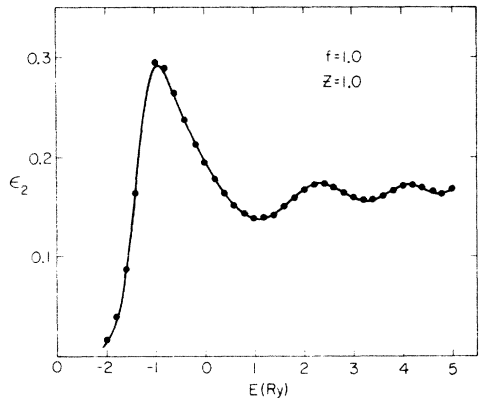

FIG. 7. The absorption function ϵ_2 as a function of energy, for unit field ($f=1$) and unit charge ($Z=1$). Points: present theory; solid line: numerical results.

limit of an exciton with negligible electron-hole interaction ($Z=0$)].

Figures 7 and 8 exhibit $\epsilon_2(E)$ for a hydrogenic atom ($Z=1$) in unit field ($f=1$). Observe the slight curvature in Fig. 8, which shows that for sufficiently large fields the absorption edge is not a perfectly exponential function of E [in the ultrastrong-field limit, $f \gg 1$, we have considerable curvature: $\epsilon_2(E;f) = (C_1 f/E)\ \exp(C_2 E^{3/2}/f)$].[25]

The negligible-binding ($Z=0$) Franz-Keldysh values of ϵ_2 are presented for unit field ($f=1$) in

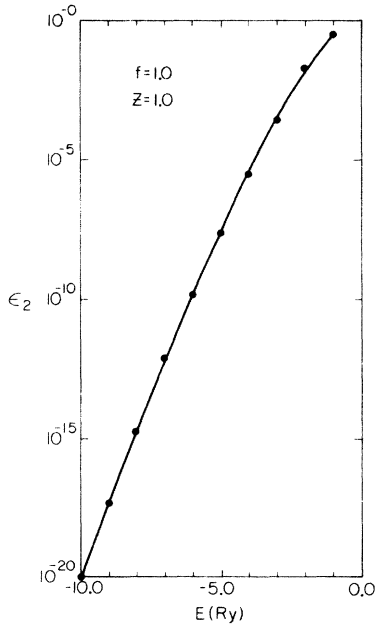

FIG. 8. The logarithm of the abosorption function ϵ_2 as a function of energy E in the negative energy (absorption edge) region. Points: present theory; line; numerical results.

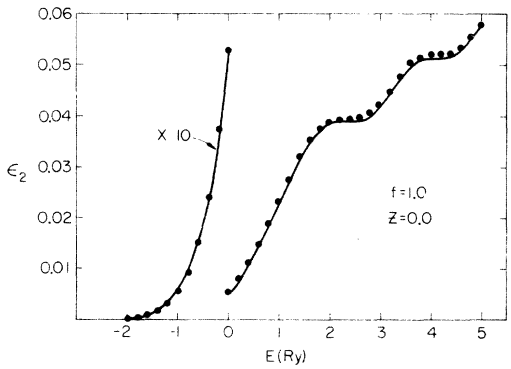

FIG. 9. The absorption function ϵ_2 as a function of energy, for the case of zero nuclear charge (Franz-Keldysh limit) and unit field. Points: current theory; line: numerical result.

Fig. 9; and the hydrogenic 1s Stark shift ($Z=1$, $f \ll 1$) is reproduced in Fig. 10. Finally, the strong-field ($f=61$) absorption by excitons ($Z=1$) is depicted in Fig. 11.

In all cases, the agreement of our approximate results with exact numerical calculations is excellent. This particular method yields excellent values of $\epsilon_2(E)$ both for weak, strong, and ultrastrong fields, and for $Z=0$ and $Z=1$. To our knowledge, no other non-numerical approximation scheme even reproduces the peaks of $\epsilon_2(E;f)$ at the correct energies, for both weak and ultrastrong fields f.

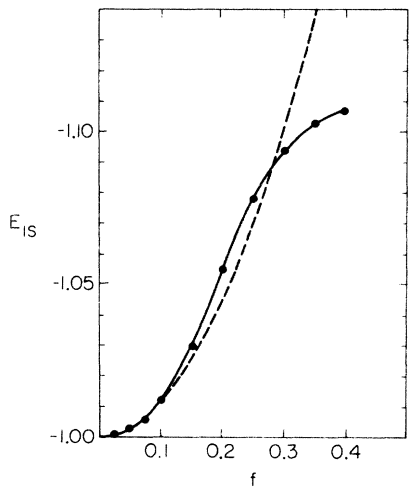

FIG. 10. The energy at which the 1s hydrogenic resonance occurs, as a function of the applied electric field f. The dashed line represents the perturbation-theory formula $E_{1s} = -1 - \frac{9}{8} f^2$, whereas the points and the solid line are the result of the present theory and numerical calculations, respectively. For low fields ($f \leq 0.1$) the present theory agrees with perturbation theory, but for higher fields the perturbation result becomes inaccurate whereas the present theory does not.

VI. CONCLUSION

The approximate electric field perturbed wave functions [Eqs. (3.4) and (4.5)] accurately reproduce the exact hydrogenic optical-absorption function $\epsilon_2(E;f)$ throughout the interesting ranges of energy E and field strength f, and therefore provide an accurate but analytically simple description of hydrogenic atoms in a field of arbitrary strength. Future theoretical work on the ultrastrong-field Stark effect should concentrate on increasing the simplicity of the present piecewise-continuous wave functions without sacrificing their accuracy.

APPENDIX A: BOUND-STATE OUTER SOLUTION

The bound-state outer solutions are constructed piecewise from WKB-like solutions first proposed by Imai.[22] The Imai solutions $\theta(u)$ are defined via a Schrödinger equation

$$[(d^2/du^2) - W_1(u)]\Theta(u) = 0 , \tag{A1}$$

with the potential $W_1(u)$, which has a zero at u_1 and the expansion near u_1:

$$W_1(u) = a_1(u-u_1) + a_2(u-u_1)^2 + a_3(u-u_1)^3 + a_4(u-u_1)^4 + \cdots . \tag{A2}$$

One defines two quantities λ and κ:

$$\lambda = \frac{12}{35}\frac{3a_2^2 - 5a_1a_3}{[2a_1^2]^{4/3}} \tag{A3}$$

$$\kappa = 1 - \frac{4}{75}\frac{14a_2^3 - 35a_1a_2a_3 + 25a_1^2a_4}{a_1^4} . \tag{A4}$$

The Imai solutions[18] of Eq. (A1) are

$$\Theta_1^I(u_1:u) = [S_1(u)/E_{k1}(u)]^{1/4}\,\mathrm{Ai}(-V_1(u)) \tag{A5}$$

and

$$\Theta_2^I(u_1:u) = [S_1(u)/E_{k1}(u)]^{1/4}\,\mathrm{Bi}(-V_1(u)) , \tag{A6}$$

where we have

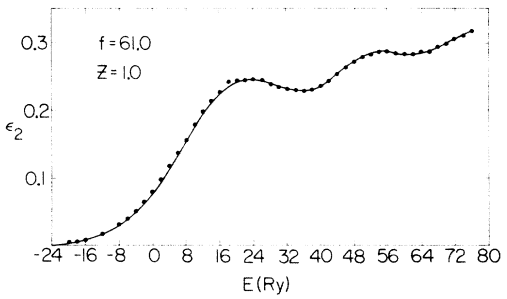

FIG. 11. The absorption function ϵ_2 as a function of energy E, for unit charge ($Z=1$) and a large reduced field ($f=61$). Points: present theory; line: numerical results.

$$S_1(u) = \left[\tfrac{3}{2}\int_{u_1}^{u} |E_{k1}(y)|^{1/2}dy\right]^{2/3} \mathrm{sgn}(E_{k1}(u)) , \tag{A7}$$

$$V_1(u) = a + bS_1(u) , \tag{A8}$$

$$b = \kappa^{2/3} , \tag{A9}$$

$$a = \lambda/(\kappa^{4/3}2^{2/3}) , \tag{A10}$$

and Ai and Bi are Airy functions. For the case that κ differs significantly from unity, the above solutions become inaccurate and one utilizes the Langer solutions

$$\Theta_1^L(u_1:u) = [S_1(u)/E_{k1}(u)]^{1/4}\,\mathrm{Ai}(-S_1(u)) \tag{A11}$$

and

$$\Theta_2^L(u_1:u) = [S_1(u)/E_{k1}(u)]^{1/4}\,\mathrm{Bi}(-S_1(u)) . \tag{A12}$$

Define the functions Θ_1 and Θ_2, which reduce to the Imai and Langer solutions in the appropriate limits:

$$\Theta_1(u_1:u) = [S_1(u)/E_{k1}(u)]^{1/4}\,\mathrm{Ai}(-V_1'(u)) \tag{A13}$$

and

$$\Theta_2(u_1:u) = [S_1(u)/E_{k1}(u)]^{1/4}\,\mathrm{Bi}(-V_1'(u)) , \tag{A14}$$

where we have

$$V_1'(u) = (\kappa')^{2/3}\left(S_1(u) + \frac{\lambda'}{(\kappa')^2 2^{2/3}}\right) . \tag{A15}$$

Here we have

$$\kappa' = \kappa,\ \lambda' = \lambda \quad \text{if } \kappa > 0 \text{ and } u_1 > 1.1 \tag{A16}$$

$$\kappa' = 1,\ \lambda' = 0 \quad \text{if } \kappa < 0 \text{ or } u_1 < 0.9 \tag{A17}$$

$$\left.\begin{aligned}\kappa' &= 1 + 5(\kappa - 1)(u_1 - 0.9)\\ \lambda' &= 5\lambda(u_1 - 0.9)\end{aligned}\right\} \text{if } \kappa > 0 \text{ and } 0.9 < u_1 < 1.1 \tag{A18}$$

and Θ_1 and Θ_2 are accurate solutions of Eq. (A1) for any λ and κ.

An examination of the bound-state effective potential $W_1(u)$ reveals that $W_1(u)$ may have either one or three (not necessarily distinct) roots (see Fig. 1). For the case that there is one root u_1, the outer solutions are given by

$$F_N^{\mathrm{out}}(u, E', \tau) = \Theta_1(u_1:u) , \tag{A19}$$

$$G_N^{\mathrm{out}}(u, E', \tau) = \Theta_2(u_1:u) . \tag{A20}$$

For the case that there are three roots u_1, u_2, and u_3, where $u_1 > u_2 > u_3$, and two extrema u_1^0 and u_2^0, where $u_1^0 > u_2^0$, the solutions have the form

$$F^{\mathrm{out}}(u, E', \tau) = \begin{cases} \Theta_1(u_1:u), & u > u_1^0 \\ A_1\Theta_1^L(u_2:u) + B_1\Theta_2^L(u_2:u), & u_1^0 > u > u_2^0 \\ C_1\Theta_1^L(u_3:u) + D_1\Theta_2^L(u_3:u), & u_2^0 > u \end{cases} \tag{A21}$$

and

$$G^{\text{out}}(u, E', \tau) = \begin{cases} \Theta_2(u_1{:}u), & u > u_1^0 \\ A_2\Theta_1^L(u_2{:}u) + B_2\Theta_2^L(u_2{:}u), & u_1^0 > u > u_2^0 \\ C_2\Theta_1^L(u_3{:}u) + D_2\Theta_2^L(u_3{:}u), & u_2^0 > u\,. \end{cases} \tag{A22}$$

The coefficients $A_1, B_1, C_1, D_1, A_2, B_2, C_2$, and D_2 are chosen to make F and G and their derivatives continuous at u_1^0 and u_2^0.

APPENDIX B: CONTINUUM OUTER SOLUTIONS

The outer solutions of the continuum equation, K^{out} and L^{out}, are constructed piecewise from WKB-like solutions in a manner analogous to that for the bound-state solutions F^{out} and G^{out}. However, the construction of accurate outer solutions is rendered somewhat simpler by the fact that $W_2(v)$ always has exactly one maximum (for $m=0$). $W_2(v)$ has either zero or two (not necessarily distinct) classical turning points $[W_2(v)=0]$ (see Fig. 2).

In the case of zero classical turning points, the ordinary WKB wave functions are adequate for our purposes. Therefore we have

$$K^{\text{out}} = \frac{1}{\sqrt{\pi}} \frac{1}{[-W_2(v)]^{1/4}} \sin\left(P_2(v) + \frac{\pi}{4}\right) \tag{B1}$$

and

$$L^{\text{out}} = \frac{1}{\sqrt{\pi}} \frac{1}{[-W_2(v)]^{1/4}} \sin\left(P_2(v) + \frac{\pi}{4}\right), \tag{B2}$$

where

$$P_2(v) = \int_{v_0}^{v} |W_2(v')|^{1/2} dv' \tag{B3}$$

is the WKB phase integral and v_0 is the value of v at which the maxima of $W_2(v)$ occurs.

For the case of two turning points we take over the functions Θ_1 and Θ_2 defined in Appendix A, first substituting $E_{k2}(v)$ for $E_{k1}(u)$ in Eqs. (A1) and (A2). The functions $\Theta_1(v_1{:}v)$ and $\Theta_2(v_1{:}v)$ then take the form

$$\Theta_1(v_1, v) = [S_2(v)/E_{k2}(v)]^{1/4}\,\text{Ai}(-V_2'(v))\,, \tag{B4}$$

$$\Theta_2(v_1, v) = [S_2(v)/E_{k2}(v)]^{1/4}\,\text{Bi}(-V_2'(v))\,, \tag{B5}$$

where we have

$$S_2(v) = \left[\tfrac{3}{2}\int_{v_1}^{v} |E_{k2}(y)|^{1/2}\, dy\right]^{2/3} \text{sgn}(E_{k2}(v)) \tag{B6}$$

and $$V_2'(v) = (\kappa')^{2/3}\left(S_2(v) + \frac{\lambda'}{(\kappa')^2 2^{2/3}}\right). \tag{B7}$$

Here we have

$$\kappa' = \kappa \text{ and } \lambda' = \lambda \text{ if } \kappa > 0.25\,, \tag{B8}$$

$$\kappa' = 1 \text{ and } \lambda' = 0 \text{ if } \kappa < 0.25\,. \tag{B9}$$

Now if v_1 and v_2 are the two turning points, if we have $v_1 > v_2$, and if v_0 is the maximum of W_2, then the functions K^{out} and L^{out} are given by

$$K^{\text{out}}(v, E', Z') = \begin{cases} \Theta_1(v_1, v), & v > v_0 \\ A_3\Theta_1(v_2, v) + B_3\Theta_2(v_2, v), & v < v_0 \end{cases} \tag{B10}$$

and

$$L^{\text{out}}(v, E', Z') = \begin{cases} \Theta_2(v_1, v), & v > v_0 \\ C_3\Theta_1(v_2, v) + D_3\Theta_2(v_2, v), & v < v_0\,. \end{cases} \tag{B11}$$

Here A_3, B_3, C_3, and D_3 are chosen to make K^{out}, L^{out}, and their derivatives continuous at v_0.

---

*Research supported by the National Science Foundation under Grant No. NSF-GH-33634.

†National Science Foundation Trainee.

[1] T. Kato, *Perturbation Theory for Linear Operators*, Die Grundlagen der Mathematischen Wissenschaften in Einzeldarstellungen (Springer-Verlag, New York, 1966), Vol. 132.

[2] H. Rausch von Traubenberg and R. Gebauer, Z. Phys. 54, 307 (1929); Z. Phys. 56, 254 (1929).

[3] J. R. Oppenheimer, Phys. Rev. 31, 66 (1928).

[4] J. Bardeen, Phys. Rev. Lett. 6, 57 (1961); M. H. Cohen, L. M. Falicov, and J. C. Phillips, Phys. Rev. Lett. 8, 316 (1962).

[5] C. Lanczos, Z. Phys. 62, 518 (1930); Z. Phys. 65, 431 (1930); Z. Phys. 68, 204 (1931).

[6] M. H. Rice and R. H. Good, J. Opt. Soc. Am. 52, 239 (1962).

[7] J. Bekenstein and J. Krieger, Phys. Rev. 188, 136 (1969).

[8] L. B. Mendelsohn, Phys. Rev. 176, 90 (1968).

[9] M. Alexander, Phys. Rev. 178, 34 (1969).

[10] J. O. Hirschfelder and L. A. Curtiss, J. Chem. Phys. 55, 1395 (1971).

[11] R. Riddell, thesis (University of California, Berkeley, 1965) (unpublished).

[12] C. B. Duke and M. E. Alferieff, Phys. Rev. 145, 583 (1966).

[13] W. Franz, Z. Naturforsch, 13a, 484 (1958); L. V. Keldysh, Zh. Eksp. Teor. Fiz. 34, 1138 (1958) [Sov. Phys.—JETP 7, 788 (1958)]; B. O. Seraphin, in *Semiconductors and Semimetals*, edited by R. K. Willardson and A. Beer (Academic, New York, 1970), Vol. VI.

[14] J. D. Dow and D. Redfield, Phys. Rev. B 1, 3358 (1970).

[15] L. J. Sham and T. M. Rice, Phys. Rev. 144, 708 (1966).

[16] H. I. Ralph, J. Phys. C 1, 378 (1968).

[17] D. F. Blossey, Ph.D. thesis (University of Illinois,

1969) (unpublished); Phys. Rev. B 2, 3976 (1970).
[18]John D. Dow, Surf. Sci. 37, 786 (1973).
[19]B. Lao, J. Dow, and F. Weinstein, Phys. Rev. B 4, 4424 (1971).
[20]E. Schrödinger, Ann. Phys. (Leipz.) 80, 457 (1926); P. S. Epstein, Phys. Rev. 28, 695 (1926); V. Fock, Z. Phys. 98, 145 (1935); V. Bargmann, Z. Phys. 99, 576 (1936).
[21]H. A. Kramers, *Quantenthearie des Elektrons und der Strahlung* [*Quantum Mechanics* (Dover, New York, 1964), pp. 306–307].
[22]I. Imai, Phys. Rev. 74, 113 (1948).
[23]See Refs. 14 and 16 for a discussion of the numerical technique.
[24]The error is somewhat larger for large negative $\tau(E')$, a region of little importance.
[25]K. Tharmalingam, Phys. Rev. 130, 2204 (1963).